

Exaggerated Shading for Depicting Shape and Detail

Szymon Rusinkiewicz
Princeton University

Michael Burns
Princeton University

Doug DeCarlo
Rutgers University

Abstract

In fields ranging from technical illustration to mapmaking, artists have developed distinctive visual styles designed to convey both detail and overall shape as clearly as possible. We investigate a non-photorealistic shading model, inspired by techniques for cartographic terrain relief, based on dynamically adjusting the effective light position for different areas of the surface. It reveals detail regardless of surface orientation and, by operating at multiple scales, is designed to convey detail at all frequencies simultaneously.

Keywords: Non-photorealistic rendering, shape depiction

1 Introduction

This paper investigates the problem of *communicating* surface geometry to viewers, including both overall shape and fine-scale detail. With standard rendering methods, based on local lighting or global illumination, it may be difficult to depict detail everywhere on a surface, since fine structure is typically revealed only with grazing lighting (i.e., when the light is near the horizon, as seen by a portion of the surface). Interactive systems that permit the lighting and/or view to be controlled by the user allow for better exploration, but *non-photorealistic* methods can be used to increase the amount of information conveyed by a single view. In fact, it is common for artists of technical drawings, medical illustrations, and shaded topographical relief to depict surfaces in a way that is inconsistent with any physically-realizable lighting model [Imhof 1982], but that is specifically intended to bring out the most detail.

Inspired by techniques used in cartography to produce shaded relief drawings of terrain, we develop a non-photorealistic rendering strategy based on multiscale local toon shading. This combines three key ideas:

- The lighting is clamped as in a toon shader to emphasize large bends in the surface, as opposed to gradual changes in slope (in practice we implement a “soft” clamping to avoid spurious visual discontinuities).
- The lighting is computed at multiple scales (using surface normals smoothed by different amounts) in order to simultaneously convey overall shape and details at different frequencies. The user can control the relative emphasis given to different scales, to yield the desired effect.
- The light direction varies such that it is always “grazing” with respect to the overall orientation of that part of the object, thus bringing out detail (Figure 1).

Taking inspiration from an examination of some of the principles of shaded relief (Section 2), we describe our rendering algorithm (Section 3) with the three stages outlined above, as well as extensions (Section 4) including curvature-based light placement, variation of detail for controlling attention, and volumetric rendering. We demonstrate the shading method in an interactive application, with user control over viewpoint and overall lighting direction, and propose applications ranging from displaying fine detail, such as

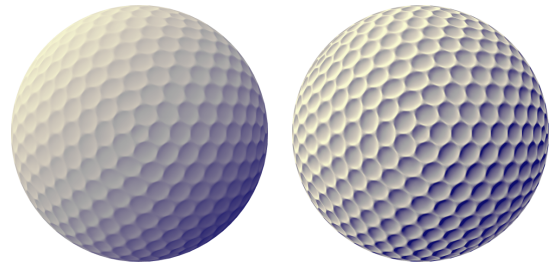


Figure 1: Simple diffuse lighting (left) results in lower contrast in the upper-left and lower-right regions of this golf ball, where the surface is facing towards or away from the light. Our proposed exaggerated shading (right) brings out detail throughout the surface by locally moving the light direction to be grazing with respect to the surface. While this example shows greatly increased contrast, a user could adjust the parameters of our model to produce a more subtle effect.

chisel marks, to intuitive visualization of the results of geometric signal processing algorithms. We compare our work (Section 5) to several existing techniques for nonphotorealistic depiction of shape.

2 Principles of Shaded Relief

Our method for detail depiction is inspired by principles of hand-shaded terrain relief that have been developed over the years. Even though a great deal of artistry is required, cartographers such as Eduard Imhof [1982] and Tom Patterson [shadedrelief.com] have articulated some of the general principles involved:

1. Shadows and specular reflections should be omitted.
2. The lighting should appear to originate, broadly speaking, from the top of the image. Illumination from the “northwest” (upper-left) is commonly used.
3. The direction from which light appears to originate can be locally adjusted. For example, if a mountain ridge curves slightly, one side of the ridge should continue to be lighter while the other is dark. Similarly, given mountain ridges running at different orientations with respect to the “global” light direction, their “light” sides should have the same brightness, as should their “dark” sides.
4. The height should be exaggerated, and there should be sharp transitions in brightness at ridges and valleys.
5. When generating relief drawings using a computer, Patterson suggests blending between renderings made using the original geometry and a smoothed version.

In addition to these, there are other principles used by artists that we do not attempt to emulate, including selective shape generalization, atmospheric perspective (a fog-like effect), hypsometric tinting, manual adjustment of shapes for visual consistency, and occasional dramatic warping of the source geometry. (In some extreme examples, we have seen an entire mountain range rotated to lie parallel to the edge of the paper!) Figure 2, left, shows an example of hand-drawn shaded relief of the area around Mt. Rainier, in Washington state, U. S.

Although we develop an algorithm for depiction of general 3D shapes (rather than just height fields), we adopt several ideas based on the above guidelines. For example, we vary the effective position of the light source throughout the scene, and compute the shading at multiple scales in order to bring out detail while also conveying overall shape.



Produced by U. S. National Park Service, public domain.

Hand-drawn shaded relief

Our method, starting from 40-meter elevation data

Figure 2: Our shading method is inspired by hand-made drawings of terrain relief, as shown at left. At center, we show the output of our method, with parameters chosen to roughly resemble the image at left. While we do not reproduce the style exactly (particularly in the depiction of the snowcap), the pattern of light and dark is the same. At right, we show the flexibility of our method: with a few changes to parameters, this rendering reveals more detail.

3 Shading Algorithm

Local lighting model: We begin by restricting ourselves to terrain data (i.e., height fields), and considering the lighting model to be used at a single scale. In his classic work on hill shading, Horn [1981] describes several models that could be employed, but we start with simple Lambertian shading based on the dot product between the surface normal and light source. In order to provide detail in regions that would ordinarily be self-shadowed, we consider “unclamped” cosine shading with an ambient term:

$$\frac{1}{2} + \frac{1}{2} \hat{n} \cdot \hat{l}, \quad (1)$$

where the circumflex or “hat” denotes vectors normalized to unit length. The light source direction l points “northwest,” or towards the upper left of the image (following principle #2 above).

In order to emphasize local detail, a frequently-used method is to exaggerate height (principle #4), as shown in Figure 3, center. As the amount of exaggeration increases, the result eventually approaches *aspect shading*, in which brightness is solely a function of the azimuth of the normal. While this achieves the goal of emphasizing small slopes, it remains the case that ridges running in some directions have greater contrast than others. For example, Figure 3 illustrates a (synthetic) height field dataset containing a series of ridges radiating from a central hill. Even with height exaggeration, ridges running close to northwest/southeast exhibit less contrast than northeast/southwest ridges.

For this reason, we adopt a method inspired by cartoon shading [Decaudin 1996], in which the results of the lighting calculation are pushed towards pure white and black. Specifically, we use a “soft toon” shader:

$$\frac{1}{2} + \frac{1}{2} \text{clamp}_{[-1\dots 1]} a(\hat{n} \cdot \hat{l}), \quad (2)$$

where a is a user-selected “exaggeration” parameter (typically between 25 and 50 for the examples in this paper). As shown in Figure 3, right, this retains the property of emphasizing sloped (as opposed to horizontal) surfaces, but ridges of almost all orientations now receive approximately the same emphasis (principle #3). The use of a soft transition (as opposed to simply snapping to black or white) preserves an intermediate tone for perfectly level terrain.

Multiscale shading: We perform the above lighting calculation at multiple scales (principle #5), with each shading pass using successively smoother geometry. In practice, we smooth the surface normal field rather than the shape itself. Specifically, for each vertex we store the original surface normals (which we will refer to as n_0), as well as several smoothed versions (denoted n_i , for $i = 1..b$) that are computed as a preprocess. The smoothing is performed by computing a weighted average of nearby normals for each vertex,

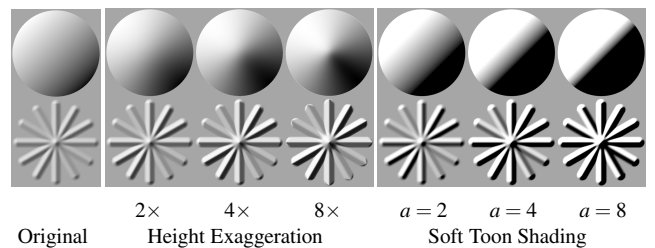


Figure 3: Local lighting models, as illustrated on a sphere and a series of ridges radiating from a central peak. **Left:** diffuse shading. **Center:** a frequently-recommended strategy for emphasizing detail in terrain renderings is scaling the height. **Right:** we instead adopt a shading model (equation 2) based on soft toon shading. In addition to emphasizing detail, this strategy also equalizes contrast between ridges running in different directions. Of course, this strategy would still fail for a perfectly northwest-southeast ridge.

weighted by a Gaussian falloff and the Voronoi area [Meyer et al. 2002] of each vertex. The Gaussian widths used for the averaging are a geometric series, with each round of smoothing having its width σ_i a constant factor times the previous width σ_{i-1} (a factor of $\sqrt{2}$ appears to work well in all cases).

Given the smoothed normals, we perform a series of shading calculations using each set in turn. The results are then combined together, with a final multiplier and offset of $1/2$ used to remap the values to the range $[0..1]$, as in equation (1).

Extension to arbitrary geometry — local lighting: To extend our terrain shading algorithm to arbitrary 3D objects, we cannot use a single light source direction: this would provide less detail in areas of the surface facing directly towards or away from the light, with more detail visible with grazing light. Therefore, we adjust the local light direction *per vertex* and *per scale*, according to the normals in the next smoother scale. As shown in Figure 4, this is done by projecting the light source direction into the plane perpendicular to the smoothed normal n_{i+1} , then computing our soft toon shading using this light direction and the original normal:

$$c_i = \text{clamp}_{[-1\dots 1]} a(\hat{n}_i \cdot \hat{l}_{i+1}), \quad (3)$$

where

$$l_{i+1} = l_{global} - \hat{n}_{i+1} (\hat{n}_{i+1} \cdot l_{global}). \quad (4)$$

This places the light at the horizon relative to the smoothed normal, and thus emphasizes local detail regardless of overall surface orientation. This is similar in spirit to building a Laplacian image pyramid by computing differences between images smoothed by

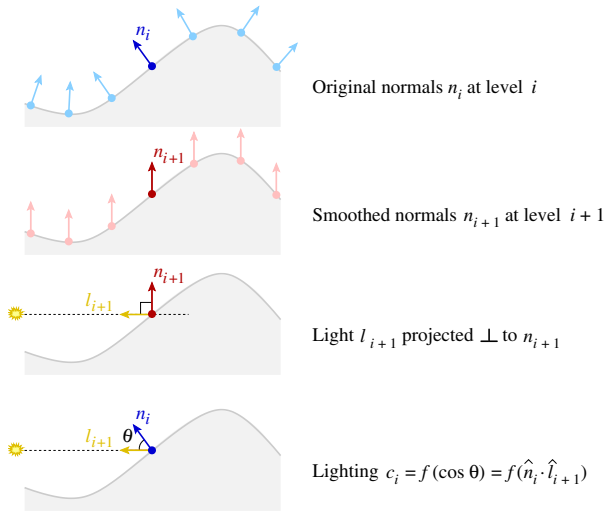


Figure 4: For rendering arbitrary 3D geometry, the effective light source direction is adjusted on each pass to lie in the plane perpendicular to the next-smoother normal.

successively-larger Gaussians, and also resembles the multiresolution thresholded “brightness” computation of Gooch et al. [2004].

The results of these lighting calculations at all scales are combined with a global offset and simple unclamped-cosine shading for the lowest level of detail:

$$c = \underbrace{\frac{1}{2} + \frac{1}{2} \left(k_b (\hat{n}_b \cdot \hat{l}_{global}) \right)}_{\text{“Base coat”}} + \underbrace{\sum_{i=0}^{b-1} k_i c_i}_{\text{“Detail terms”}}. \quad (5)$$

The contributions of the multiple passes are illustrated in Figure 5. Note that the detail terms are *signed*, so the figure illustrates them with a multiplier and offset of $1/2$.

Stylistic control: There are a few user-tunable parameters that affect the appearance of the final result:

- The total number of scales of smoothing or “frequency bands,” denoted as b , affects the range of scales of detail that are depicted. It should be related to the size of the finest surface features, relative to the size of the entire model. The examples in this paper use values of b between 8 and 13.
- The contribution of each scale, k_i , affects whether high or low frequencies will be emphasized, or whether all scales contribute equally. We have found that making k_i proportional to a power of the smoothing width σ_i provides intuitive control: a single slider can affect which scales are emphasized (Figure 6). Effective visualizations typically result from powers between 0 (flat across frequencies) and -1 (contrast proportional to frequency), with $-1/2$ a reasonable default. The k_i are normalized to sum to 1, or any other constant (determining overall contrast).
- The final color c may be remapped using any colormap, including ones that apply gamma correction or introduce color variation. It is also possible to combine the images resulting from different “global” lighting directions, by using a 2D colormap indexed by values of c computed using different l_{global} . A number of possibilities are presented in Figure 7, while Figure 1 uses a yellow-to-blue mapping inspired by Gooch et al. [1998].

4 Extensions

Principal direction-based light adjustment: Our basic rendering model, described above, simply projects the light source into the plane perpendicular to the smoothed normal. We have also experimented with an effect that moves the light in that plane in order

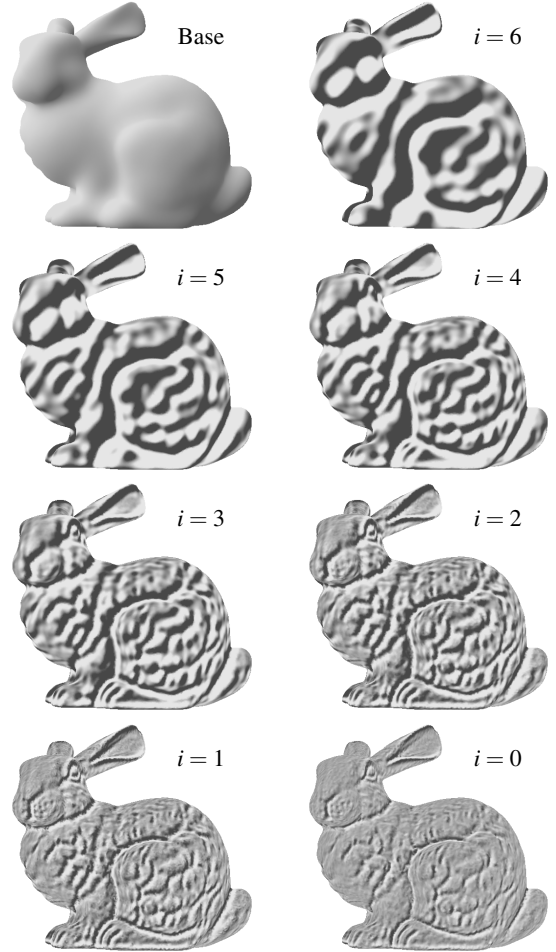


Figure 5: Our shading strategy combines terms revealing detail at multiple scales, as visualized here.

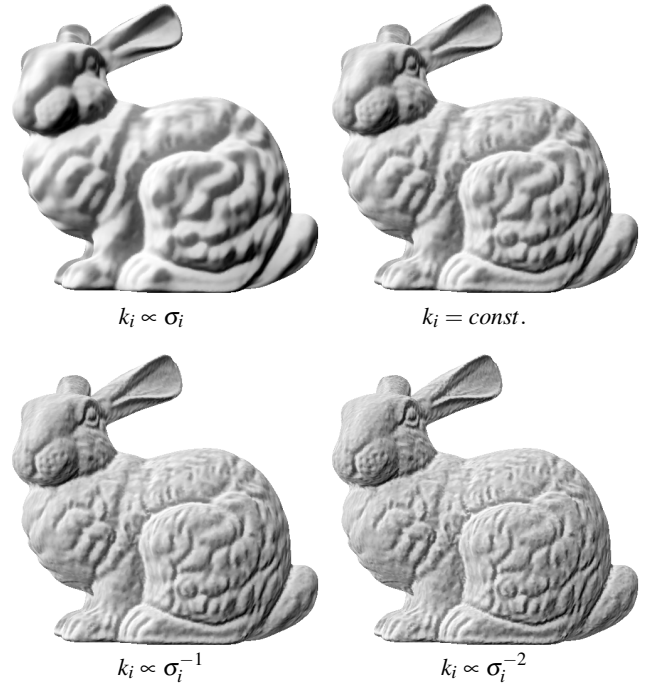


Figure 6: The relative contribution of each scale may be varied to produce different effects in the final renderings.

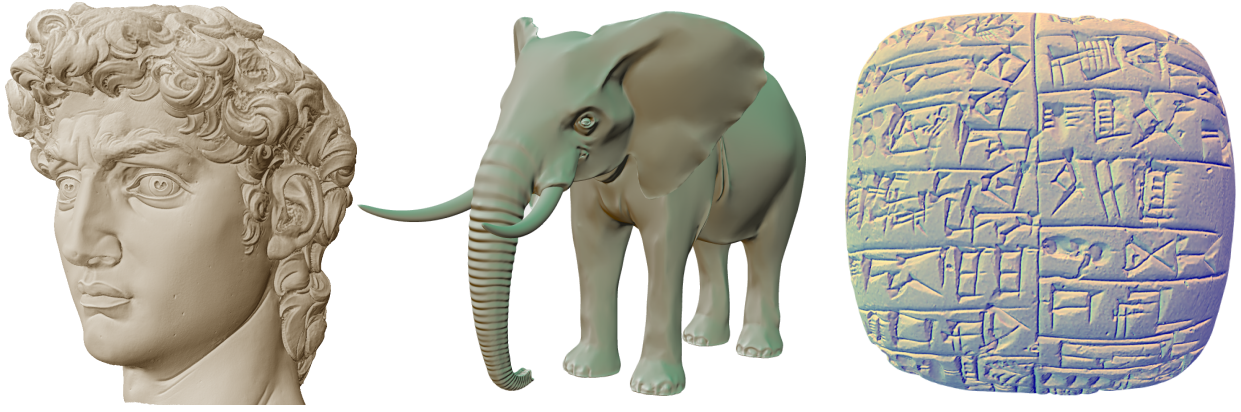


Figure 7: Examples using different colormaps. The latter two figures use two passes, with the light source placed first at northwest then at northeast.

to maximize local contrast. To derive this, we suppose the light source is in some (normalized) direction δ in the tangent plane, and compute contrast as the magnitude of the gradient of the shading:

$$\text{contrast} = \|\nabla(\hat{n} \cdot \delta)\|. \quad (6)$$

Using basic identities from differential geometry [do Carmo 1976], we can show that this is equal to

$$\|\Pi \delta\| = \sqrt{2H\kappa_\delta - K}, \quad (7)$$

where Π is the second fundamental tensor, H is mean curvature, K is Gaussian curvature, and κ_δ is the normal curvature in the direction δ . This is maximized when the magnitude of κ_δ is as large as possible, which occurs when δ lies along d_1 , the principal direction corresponding to the largest-magnitude principal curvature.

Therefore, we know that maximum contrast is achieved by positioning the light source to lie along the first principal direction at each point. There is, however, an ambiguity we must resolve: the principal direction is defined only up to a 180° flip. A simple strategy, such as always choosing the flip that lies closer to the *global* light direction, leads to objectionable visual discontinuities. We eliminate these by scaling the contribution of the principal direction according to its dot product with the projected light direction:

$$l_{\text{effective}} = (d_1 \cdot l)d_1 + l. \quad (8)$$

This has the effect of reverting to the projected light direction if the principal direction is perpendicular to it, otherwise “nudging” the light source towards d_1 .

Even with this correction, there is still another possible source of visual discontinuities: locations where the principal curvatures have nearly equal magnitude. In this case, the principal direction with greatest curvature magnitude may differ by 90° between nearby surface locations. We eliminate this discontinuity by scaling the contribution of the principal direction by an amount that approaches zero as the principal curvatures become equal in magnitude:

$$l_{\text{effective}} = s(\kappa_1^2 - \kappa_2^2)(d_1 \cdot l)d_1 + l, \quad (9)$$

where s controls the strength of the principal direction adjustment. This constant should have dimensions of length squared, and we set it proportional to σ_f^2 .

The primary effect of the above light source adjustment is to increase the sharpness of brightness transitions at ridges and valleys. Figure 8 shows a comparison between purely projection-based lighting and lighting adjusted by principal curvature direction: note the increased definition of the indicated valley. We have observed that the difference is most significant near sharp creases in the surface, and for many models there is little effect.

Attention-based modulation of detail: Because one of the requirements for our shading model is a set of pre-smoothed versions of the mesh’s normals, it is simple to produce effects that vary the

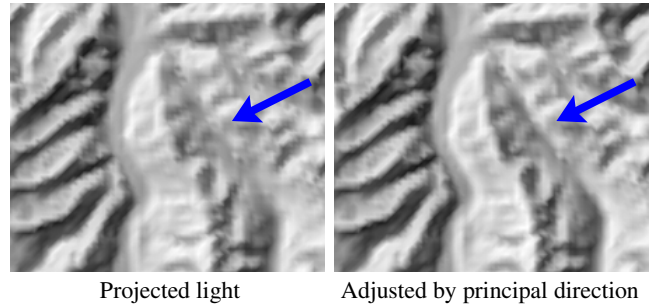


Figure 8: An example of the increased contrast along ridges and valleys produced by principal direction-based adjustment of local light direction.



Figure 9: Attenuating high-frequency detail away from a user-specified point of interest can draw attention to a specific part of the model. At right, the point of interest has been placed on the face.

relative amount of emphasis given to different frequencies at different points in the image. Figure 9 shows an example of spatially modulating the contributions of different detail passes to emphasize a point of interest. The weight of each scale band falls off away from a user-specified center of attention, with the weight of higher frequencies decreasing more rapidly. The center and amount of modulation may be manipulated interactively.

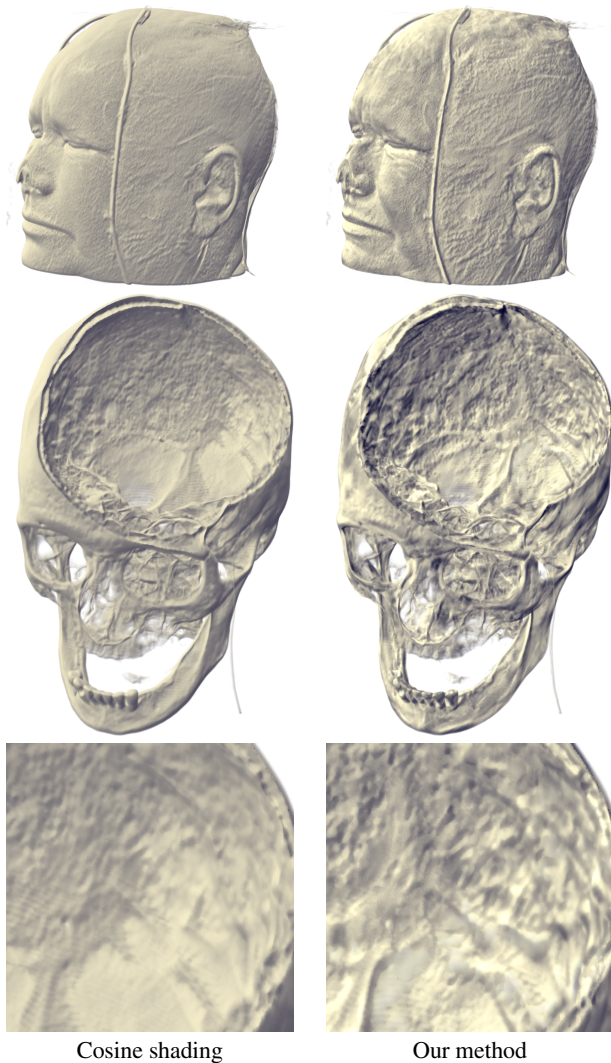


Figure 10: Volumetric renderings of the Visible Female CT dataset show increased definition in facial features (above) and ridges on the interior of the skull (below) using our shading method.

Volumetric rendering: Although we focus mostly on rendering polygonal surfaces, we believe that the proposed shading model has applications in volumetric rendering domains, such as medical visualization. Since our only requirement is a set of smoothed normal maps, which may be computed from filtered versions of the volume gradient field, we can use our model in any standard volumetric renderer. For example, Figure 10 shows images generated in a conventional slice-based volume renderer, with opacity controlled using a transfer function. At right, we augment the rendering with our shading model, with normals at each scale computed from the smoothed surface gradient. Note that our method accentuates both large-scale features (e.g., the cheek in the top renderings) and small-scale details of the model.

5 Discussion

Applications: The fine-scale surface details visualized effectively by exaggerated shading are most frequently present in either 3D scanned models or the results of geometric signal processing algorithms. Figure 12 illustrates an application that combines both of these: scanned 3D models of faces are acquired (a and b), and their detail statistics are used by a texture synthesis algorithm to enable applications such as aging [Golovinskiy et al. 2006]. Our shading

model allows for easy comparison between the results of the texture synthesis (d) and a simpler method that simply adds noise (c). Another application is illustrated in Figure 13, top right: tool marks are revealed in Michelangelo’s unfinished St. Matthew sculpture.

Implementation and costs: Our shading strategy is implemented for surfaces by computing the color c per vertex (equation 5), with the final colormap applied using a texture lookup. The rendering is efficient even in software: on a 3 GHz. Pentium 4, a bunny model with 144 k faces renders at 30 frames per second for $b = 9$ scales of smoothing. We have also implemented the algorithm in a vertex shader, which increases the performance to 90 frames per second on a GeForce 6800GT. For volumetric models, we use a slice-based renderer with the lighting computed in a fragment shader; a 33-megavoxel volume renders at approximately 1 frame per second.

The greatest cost of our algorithm is the memory dedicated to storing smoothed normals. In the current implementation, normals are stored per-vertex, though it would also be possible to store filtered normal maps as textures. The memory requirements could be reduced by storing smoothed normals sparsely on the surface, perhaps by hierarchically clustering the vertices and storing a single normal at each interior node in the hierarchy. This would also dramatically reduce precomputation time, which we have not attempted to optimize (it ranges from a few seconds or minutes for small models to several hours for the terrain and David head datasets, which have 3.5 M faces and use $b = 13$ scales of smoothing).

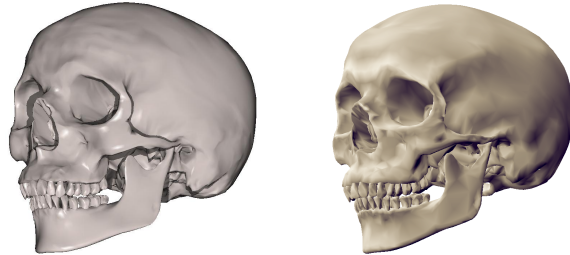
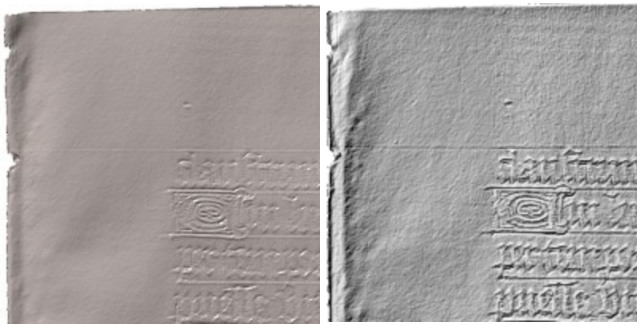
Relation to previous work: Our use of multiscale shading is related to the work of Gooch et al. [2004], who generated illustrations from single images. One component of their computation involves finding differences between successively-smoothed images, followed by thresholding. Combining filtered images, with non-linear functions applied separately to each frequency band, is also used in some approaches for tone mapping of high-dynamic-range images (e.g., [Li et al. 2005]), and it has been shown that manipulating contrast at different scales can be used to control attention in images [Su et al. 2005].

The concept of varying the light source throughout the model is related to recent work in computational photography, in which multiple photographs under different illumination are combined using either a manual painting interface or automatic criteria such as maximal contrast [Akers et al. 2003; Agarwala et al. 2004]. A similar approach is followed by the work of Lee et al. [2006], which builds upon prior work in automated lighting design [Shacked and Lischinski 2001; Gumhold 2002; Halle and Meng 2003] to place light sources that each affect small regions of the surface. Figure 11 compares our method to published results by Lee et al. [2006].

The main differences between these previous systems and our work include:

- We do not search for where to put the lights, but rather have a deterministic criterion for light positioning that allows us to compute an effective light direction *per vertex*. This allows for a temporally coherent interactive application, including the ability to change view and overall lighting direction in real time.
- Our lighting is placed according to a “global” light direction, leading to more consistent shape interpretation than with methods that light different parts of the surface independently.
- We permit the user to directly increase contrast far beyond what is possible with light source positioning. This is useful for applications involving subtle surface detail (e.g., Figure 11, top).
- The multiscale nature of our algorithm allows it to reveal details at many frequencies in a single image.

Other methods for conveying surface detail: There are comparatively few non-photorealistic rendering methods specifically designed for conveying surface detail in a single image. Among methods that operate directly on a 3D object (as opposed to performing conventional rendering then applying image processing opera-



[Lee et al. 2006]

Our method

Figure 11: Comparison of our method to published results of Geometry Dependent Lighting [Lee et al. 2006]. At top, subtle folds and slightly embossed letters are visible in a closeup of a scanned manuscript. At bottom, our method highlights ridges in this skull model.

tions), one option is the technique of Cignoni et al. [2005], who perform conventional diffuse shading using a *sharpened* normal field. This emphasizes contrast at corners, and produces effects analogous to the use of unsharp masking in photo retouching.

A second, frequently encountered, effect relies on coloring based on curvature. For example, Kindlmann et al. [2003] color convex areas of an object lighter and concave areas darker, agreeing with the intuitive observation that less light reaches valleys and folds on a surface. Closely related effects involve coloring based on accessibility [Miller 1994] or ambient occlusion [Zhukov et al. 1998], and the depth shading of Cohen et al. [2004], which all have the property that indentations on the surface are colored darker. In contrast with these approaches, our technique retains the notion of a global light source direction, and hence is inherently view-dependent. As such, it is complementary to these view-independent approaches for conveying detail. For example, our method will color one side of a valley lighter and the other darker, as opposed to darkening the valley. Figure 13 presents a comparison of our method to simple Lambertian lighting, as well as curvature and accessibility shading.

6 Conclusion and Future Work

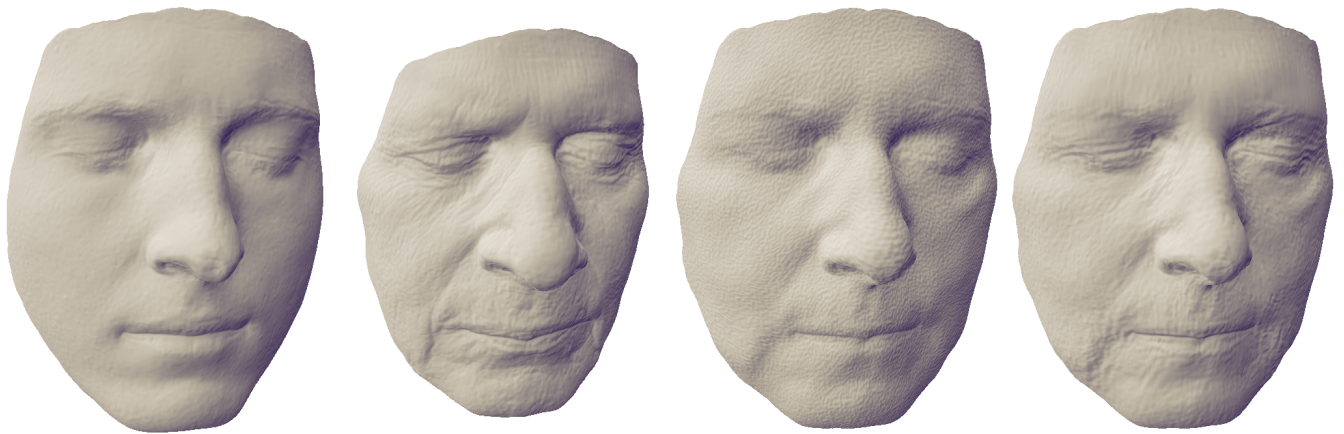
By combining multiscale processing with local adjustment to light direction, our exaggerated shading technique communicates surface geometry through single images, while also remaining practical for an interactive system. It provides an alternative to previous methods such as mean curvature shading, which often convey detail at the expense of conveying shape. Indeed, our shading model still resembles real shading, making it more readily accepted by viewers: as has been shown, the human visual system does not verify the global consistency of local estimates of illumination direction [Ostrovsky et al. 2005]. This suggests perceptual studies to investigate the amount of lighting exaggeration the human visual system can tolerate, while retaining the ability to perceive surface shape, rather than texture. Other future work includes a global optimization framework for allowing more significant changes to lighting direction while eliminating or hiding discontinuities, and an analysis of shading over continuous scale space, rather than the discrete scales we consider.

Acknowledgments

Thanks to the Tigggraph participants, especially Adam Finkelstein, for their valuable comments about this work. Models are due to Stanford, Georgia Tech, MERL, XYZRGB, de Espona, and the Visible Human project. We thank the National Science Foundation (grant CCF-0347427) and the Sloan Foundation for funding.

References

- AGARWALA, A., DONTCHEVA, M., AGRAWALA, M., DRUCKER, S., COLBURN, A., CURLESS, B., SALESIN, D., AND COHEN, M. 2004. Interactive Digital Photomontage. *ACM Trans. Graphics (Proc. SIGGRAPH)*, Vol. 23, No. 3.
- AKERS, D., LOSASSO, F., KLINGNER, J., AGRAWALA, M., RICK, J., AND HANRAHAN, P. 2003. Conveying Shape and Features with Image-Based Relighting. In *Proc. IEEE Visualization*.
- CIGNONI, P., SCOPIGNO, R., AND TARINI, M. 2005. A Simple Normal Enhancement Technique for Interactive Non-Photorealistic Renderings. *Computers & Graphics*, Vol. 29, No. 1.
- COHEN, J., DUNCAN, D., SNYDER, D., COOPER, J., KUMAR, S., HAHN, D., CHEN, Y., PURNOMO, B., AND GRAETTINGER, J. 2004. iClay: Digitizing Cuneiform. In *Proc. Symposium on Virtual Reality, Archaeology, and Cultural Heritage (VAST)*.
- DECAUDIN, P. 1996. Cartoon-Looking Redering of 3D-Scenes. Tech. Rep. 2919, INRIA.
- DO CARMO, M. P. 1976. *Differential Geometry of Curves and Surfaces*. Prentice-Hall.
- GOLOVINSKIY, A., MATUSIK, W., PFISTER, H., RUSINKIEWICZ, S., AND FUNKHOUSER, T. 2006. A Statistical Model for Synthesis of Detailed Facial Geometry. *ACM Trans. Graphics (Proc. SIGGRAPH)*, Vol. 25, No. 3.
- GOOCH, A., GOOCH, B., SHIRLEY, P., AND COHEN, E. 1998. A Non-Photorealistic Lighting Model for Automatic Technical Illustration. In *Proc. ACM SIGGRAPH*.
- GOOCH, B., REINHARD, E., AND GOOCH, A. 2004. Human Facial Illustrations: Creation and Psychophysical Evaluation. *ACM Trans. Graphics*, Vol. 23, No. 1, 27–44.
- GUMHOLD, S. 2002. Maximum Entropy Light Source Placement. In *Proc. IEEE Visualization*.
- HALLE, M., AND MENG, J. 2003. LightKit: A Lighting System for Effective Visualization. In *Proc. IEEE Visualization*.
- HORN, B. K. P. 1981. Hill Shading and the Reflectance Map. *Proc. IEEE*, Vol. 69, No. 1, 14–47.
- IMHOF, E. 1982. *Cartographic Relief Presentation*. de Gruyter.
- KINDLMANN, G., WHITAKER, R., TASDIZEN, T., AND MÖLLER, T. 2003. Curvature-Based Transfer Functions for Direct Volume Rendering: Methods and Applications. In *Proc. IEEE Visualization*.
- LEE, C. H., HAO, X., AND VARSHNEY, A. 2006. Geometry-Dependent Lighting. *IEEE Trans. Visualization and Computer Graphics*, Vol. 12, No. 2.
- LI, Y., SHARAN, L., AND ADELSON, E. H. 2005. Compressing and Companding High Dynamic Range Images with Subband Architectures. *ACM Trans. Graphics (Proc. SIGGRAPH)*, Vol. 24, No. 3.
- MEYER, M., DESBRUN, M., SCHRÖDER, P., AND BARR, A. H. 2002. Discrete Differential-Geometry Operators for Triangulated 2-Manifolds. In *Proc. VisMath*.
- MILLER, G. 1994. Efficient Algorithms for Local and Global Accessibility Shading. In *Proc. SIGGRAPH*.
- OSTROVSKY, Y., CAVANAGH, P., AND SINHA, P. 2005. Perceiving Illumination Inconsistencies in Scenes. *Perception*, Vol. 34, 1301–1314.
- PATTERSON, T. Shaded Relief: Ideas and Techniques about Relief Presentation on Maps. <http://www.shadedrelief.com/>.
- SHACKED, R., AND LISCHINSKI, D. 2001. Automatic Lighting Design using a Perceptual Quality Metric. In *Proc. Eurographics*.
- SU, S., DURAND, F., AND AGRAWALA, M. 2005. De-Emphasis of Distracting Image Regions using Texture Power Maps. In *Proc. Workshop on Texture Analysis and Synthesis*.
- ZHUKOV, S., IONES, A., AND KRONIN, G. 1998. An Ambient Light Illumination Model. In *Proc. Eurographics Rendering Workshop*.



(a) Scanned young face

(b) Scanned old face

(c) Aging+noise applied to (a)

(d) Aging+synthesis applied to (a)

Figure 12: Exaggerated shading brings out details (wrinkles and pores) in both scanned meshes and the results of aging simulation [Golovinskiy et al. 2006]. The fine-scale detail in (c) is simply noise, while (d) is the result of texture synthesis based on a spatially-varying statistical model computed from (b).



Cosine shading

Mean curvature

Accessibility

Our method

Figure 13: Comparison between detail-revealing shading effects. Note the emphasized detail in the chisel marks (top), hair (middle), and wing (bottom).